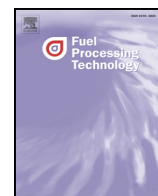




Contents lists available at ScienceDirect

## Fuel Processing Technology

journal homepage: [www.elsevier.com/locate/fuproc](http://www.elsevier.com/locate/fuproc)

# Numerical study of combustion characteristics for pulverized coal under oxy-MILD operation

Yaojie Tu, Hao Liu <sup>\*</sup>, Sheng Chen, Zhaohui Liu, Haibo Zhao, Chuguang Zheng

State Key Laboratory of Coal Combustion, Huazhong University of Science and Technology, Wuhan, Hubei 430074, China

## ARTICLE INFO

### Article history:

Received 12 July 2014

Received in revised form 3 September 2014

Accepted 18 October 2014

Available online xxxx

### Keywords:

MILD combustion

Oxy-fuel combustion

Coal combustion

Combustion modeling

NO<sub>x</sub> conversion

## ABSTRACT

MILD (Moderate or Intense Low-oxygen Dilution) combustion is a novel technology to reduce NO<sub>x</sub> emission from combustion. With the development of this technology, it is expected to combine this technology with oxy-fuel combustion to jointly control the pollutants from fossil fuel combustion. The present paper investigates the combustion characteristics of coal under oxy-MILD operation with the aid of CFD simulations. A seven-step global reaction mechanism is used for modeling coal combustion involving gaseous volumetric reaction and particle surface reaction. The predicted results using the adopted models for the reference case agree well with the experimental results. It is revealed that, the combustion temperature level increases with the enhancement of initial oxygen concentration because of the reduced injection momentum and promoted heat release. The in-furnace CO formation increases but the final CO emission reduces when enhancing the oxygen concentration under oxy-MILD combustion. Moreover, oxy-MILD combustion shows a greater potential on NO<sub>x</sub> formation reduction than air-MILD combustion, and this potential is promoted at higher initial oxygen concentration.

© 2014 Elsevier B.V. All rights reserved.

## 1. Introduction

### 1.1. MILD combustion technology and ongoing research

Moderate or Intense Low-Oxygen Dilution (MILD) combustion [1], also known as High Temperature Air Combustion (HTAC) [2], Flameless combustion or Flameless oxidation (FLOX) [3], is one of the most promising combustion technologies in the 21st century to improve thermal efficiency and reduce NO<sub>x</sub> emission. A typical characteristic of this technology is intense recirculation of combustion products inside the furnace, which on one hand dilutes both oxidizer (e.g. air, O<sub>2</sub>) and fuel streams before mixing, on the other hand preheats the reactants to above their ignition point. Therefore, several advantages have been expected such as uniform temperature distribution, decreased peak temperature, larger volume of reaction zone, and retarded NO<sub>x</sub> formation in the low oxygen partial pressure atmosphere. While it seems that the only drawback is that the furnace needs to be preheated above a relatively high temperature before MILD operation, usually in the range of 600 °C to 850 °C, which is determined by fuel types and surrounding conditions [4]. Moreover, MILD combustion provides a convenient option to combine with other advanced combustion technologies, especially oxy-fuel combustion, in order to improve the thermal efficiency remarkably

with less flue gas heat loss and significant NO<sub>x</sub> reduction [5–7], even to realize CO<sub>2</sub> capture and storage (CCS) as well [8,9].

Gaseous fuel MILD combustion has been explored for more than 20 years since the nineties of the last century, burners such as FLOX® and HRS®-NFK have been widely installed in industrial sectors [2,4,10,11]. Moreover, to further understand MILD combustion and promote its industrial application, in recent years, a great deal of efforts has been made on the fundamental issues related to regime or criterion of different combustion modes, turbulence–chemistry interactions, reactive structures and flame characteristics as well as intermediate species fields under the condition of varied fuels, different parameters and burner configurations [12–17].

### 1.2. Recent research status on coal MILD combustion

In the recent years, the corresponding reports on MILD combustion for solid fuels are still quite sparse, and the latest development of them can be found in some papers [18–34]. The International Flame Research Foundation (IFRF) has carried out a series of experiments in a 0.58 MW furnace using natural gas, heavy and light fuel oils, as well as coal since year 2000 [18–20], and the unique designed burner system consisted of a central jet of air preheated to 1623 K and two side jets for pulverized coal. Schaffel et al. [21] simulated the IFRF trials and brought forward the concepts of HTAC supercritical pulverized coal-fired boiler based on numerical simulation results of different hypothetical boiler types and dimensions [22]. Vascellari et al. [23] investigated the influence of turbulence–chemistry interaction on pulverized coal MILD combustion modeling, and claimed that Eddy Dissipation Concept (EDC) with detailed

<sup>\*</sup> Corresponding author at: State Key Laboratory of Coal Combustion, Huazhong University of Science and Technology, Wuhan, Hubei 430074, China. Tel.: +86 27 87544779 8310; fax: +86 27 87545526.

E-mail address: [liuhao@mail.hust.edu.cn](mailto:liuhao@mail.hust.edu.cn) (H. Liu).

**Table 1**  
Parameters used for the CPD Devolatilization Model [23].

Parameter	Value	Unit
Initial fraction of bridges in coal lattice	0.52	–
Initial fraction of char bridges	0	–
Lattice coordination number	5	–
Cluster molecular weight	351.2	kg/kmol
Side-chain molecular weight	33.9	kg/kmol

**Table 2**  
The physical properties (proximate and ultimate analysis) of the coal particle [21].

Proximate analysis (wt% ad.)				Ultimate analysis (wt% daf.)							LCV (MJ/kg)
Moisture (105 °C)	Ash	VM	FC	C	H	O	N	S			31.74
2.9	3.3	37.1	56.7	81.6	5.5	10.7	1.5	0.6			

kinetic mechanisms might better reproduce the chemical and fluid dynamic behavior of coal MILD combustion according to the comparison between numerical simulation results with IFRF's experimental measurements.

Suda and He et al. [24,25] investigated flame behavior, ignition delay, burnout, and NO<sub>x</sub> emission of coal under MILD combustion experimentally and numerically in a 250 kW furnace. Their results indicated that NO<sub>x</sub> concentration decreased as air temperature increased, and a lower NO<sub>x</sub> concentration was observed during high-volatile coal combustion. It was suggested that high-concentration HCN and NO near primary air exit both led to NO destruction.

An integrated burner coupling MILD combustion with air staging has been developed within the European Union supported project FLOX-COAL [26–31]. In these works, a significant reduction of NO<sub>x</sub> emission was achieved by MILD combustion [26]. The char gasification by CO<sub>2</sub> and H<sub>2</sub>O leads to an increased CO concentration in the primary combustion zone thus further reducing the O<sub>2</sub> concentration, moreover, the diluted oxygen as well as higher concentration NO-intermediates results in higher reduction of NO [27,28]. In addition, it was observed that the total NO<sub>x</sub> reduction can't be attributed to flue gas recirculation alone, while a reduced conversion of fuel-N to NO also can make some effects [31].

Our group [35,36] recently has reported an experimental study on the MILD combustion of oil and coal in a 0.3 MW pilot-scale furnace. Two arranging patterns of MILD burners were investigated including symmetrical and asymmetrical arrangements of secondary stream. The results showed that, the asymmetrical configuration produced the larger recirculation zone as well as a more uniform temperature distribution. However, the char burnout under MILD operation was found to be weaker than the conventional combustion.

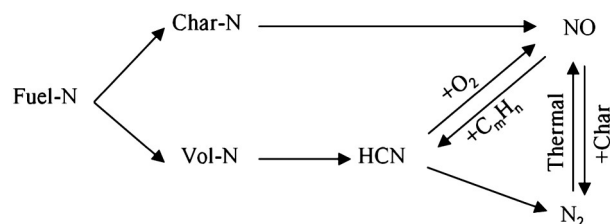
### 1.3. Objectives of the present work

Coal is an abundant fuel resource in many developing countries and still plays an important role in worldwide power generation for years to come. However, nitrogen oxides, regarded as one major pollutant from pulverized coal combustion, are receiving international concern due to

**Table 3**  
Combustion mechanism of coal used in the present study (units in SI)<sup>a</sup>.

Index	Reactions	A [kmol/(m <sup>3</sup> s <sup>-1</sup> )]	Ea (J/kmol)
R.1	$C_xH_yO_z + (x-z)/2O_2 \rightarrow xCO + y/2H_2$	$3.80 \times 10^7$	$5.55 \times 10^7$
R.2	$CO + H_2O \rightarrow CO_2 + H_2$	$2.75 \times 10^9$	$8.37 \times 10^7$
R.3	$CO_2 + H_2 \rightarrow CO + H_2O$	$6.81 \times 10^8$	$1.14 \times 10^8$
R.4	$H_2 + 0.5O_2 \rightarrow H_2O$	$9.87 \times 10^8$	$3.1 \times 10^7$
R.5	$C + CO_2 \rightarrow 2CO$	$6.35 \times 10^{-3}$	$1.62 \times 10^8$
R.6	$C + H_2O \rightarrow CO + H_2$	$1.92 \times 10^{-3}$	$1.47 \times 10^8$
R.7	$C + 0.5O_2 \rightarrow CO$	$5 \times 10^{-3}$	$7.4 \times 10^7$

<sup>a</sup> The reaction rate coefficient  $k = A \exp(-E_a/R_u T)$ , where  $R_u = 8315 \text{ J kmol}^{-1} \text{ K}^{-1}$ .

**Fig. 1.** A simplified chemical reaction path of fuel-NO formation.

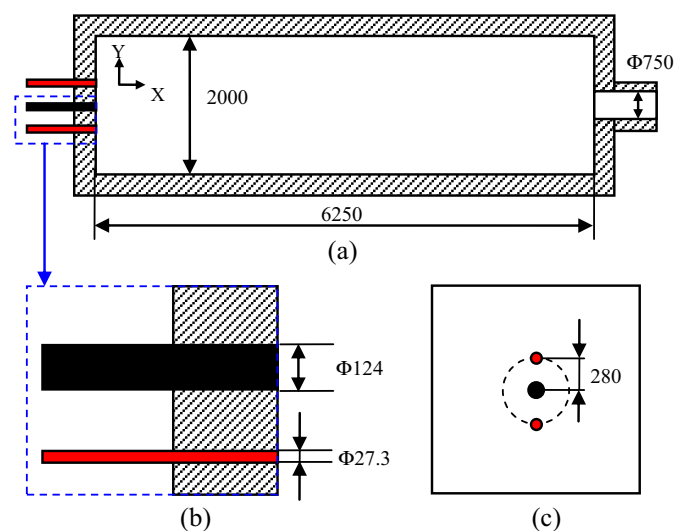
their action as precursor to acid rain and photochemical smog, especially in China. It is clear that MILD combustion has great potential to be developed for solid fuels, and the positive results obtained from previous studies promote further investigations of coal MILD combustion. Besides, MILD combustion has been successfully applied for gaseous fuel even if the oxidizer (usually air) is at ambient temperature [4,32–34]. It is encouraged that MILD combustion would be combined with the oxy-fuel combustion for joint reduction of pollutants from coal combustion, i.e. NO<sub>x</sub> and CO<sub>2</sub> as well as improving thermal efficiency.

The aim of the present study is to investigate the combustion characteristics (e.g. temperature distribution, species fields and NO<sub>x</sub> conversion) of coal under oxy-MILD operation. Five cases are modeled by CFD approaches in the present work, including air-fired MILD case (AM) and four oxy-fired MILD cases at different oxygen volume fractions varying from 21% to 30% (OM21, OM24, OM27, OM30).

## 2. Modeling methods and details

In this paper, the modeling of coal combustion was performed by the commercial CFD software Fluent, version 6.3 [37]. The finite volume discretization approach is used for structured hybrid mesh by solving the Reynolds Averaged Navier Stokes (RANS) equations. The  $k-\epsilon$  turbulence model is hired for the closure of RANS equations. The SIMPLE scheme is used for pressure–velocity coupling. The P-1 model with the weighted sum of gray gas model (WSGGM-domain-based) is used to solve the radiation and absorption among the gaseous molecules, coal particles and furnace walls.

During modeling of coal, the discrete phase model (DPM) is employed by considering the Eulerian–Lagrangian approach. The continuous phase of the gases is modeled considering the Eulerian frame, while the discrete solid phase of coal particles is solved considering

**Fig. 2.** Geometric configurations of the experimental furnace and burner: (a) furnace, (b) burner, (c) top view of furnace (unit: mm).

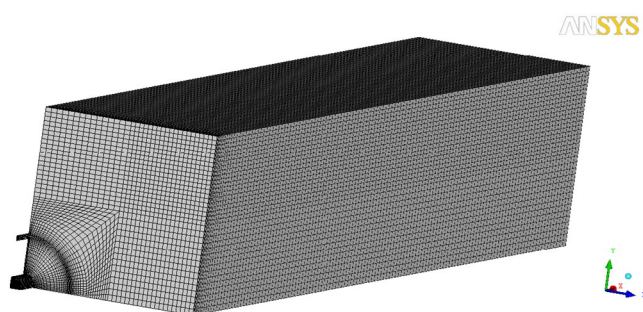


Fig. 3. Computational grid of the IFRF furnace No. 1 (1/4 geometry).

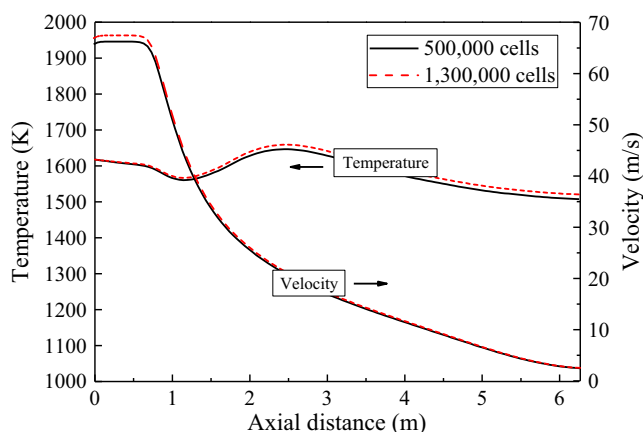


Fig. 4. Axial profiles of furnace temperature and velocity for case AM along the furnace centerline for different grid resolutions.

the Lagrangian frame. The flow pattern of continuous phase can be influenced by the discrete phase. In the following, the coal combustion models are briefly described, since the detailed description can be found elsewhere [38,39].

### 2.1. Pyrolysis and chemical reaction mechanism

The coal combustion process is assumed to be divided into three stages, namely, drying and pyrolysis of raw coal, combustion of volatiles, and burnout of char [40]. First, the release of moisture in the coal particle is governed by the vapor partial pressure difference between the particle surface and bulk surface. The evaporating temperature of the raw coal is assumed to be 400 K. The pyrolysis behavior of coal particle is evaluated with the Chemical Percolation Devolatilization (CPD) model. Table 1 presents the adopted CPD parameters used in Fluent calculations of the present coal [23]. In the modeling procedure, the pyrolysis of the coal particle is approximated by a single reaction:



The char is assumed to be pure carbon, and the pyrolysis gaseous mixture contains CO, CO<sub>2</sub>, CH<sub>4</sub>, H<sub>2</sub>O as well as other light hydrocarbon, C<sub>m</sub>H<sub>n</sub>. Similarly, the tar is considered as an equivalent molecule,

C<sub>n</sub>H<sub>m</sub>O<sub>p</sub>. In order to simplify the combustion reaction mechanism, the volatiles (mixture of tar and gas) are approximated by a single combustible species, C<sub>x</sub>H<sub>y</sub>O<sub>z</sub>, balanced to conserve stoichiometry from CPD and coal physical property analysis, which are presented in Tables 1 and 2, respectively.

Table 3 lists the combustion reaction mechanism used for the coal combustion in the present study. The homogenous reactions of the gaseous species are solved by the Eddy Dissipation Concept (EDC) model with a four step volumetric reaction mechanism (R.1–R.4). The heterogeneous reactions of the solid char are solved by a three step surface reaction mechanism (R.5–R.7). With the aid of this mechanism, Liu et al. [41] have reasonably predicted the combustion behavior of coal under conventional swirl combustion. However, whether it is appropriate for coal MILD combustion still needs further validation. Therefore, validation work of the adopted models has been conducted as described in Section 3.1

### 2.2. NO<sub>x</sub> formation

In the present work, the NO<sub>x</sub> formation is evaluated using the post-processing approach. Three formation paths together with the reduction path are considered, i.e. thermal-, prompt-, fuel-NO<sub>x</sub> and NO<sub>x</sub> reburning. The turbulence effects on temperature are considered by the probability density function (PDF). The NO<sub>x</sub> formation and destruction mechanisms are briefly described as follows.

The thermal-NO<sub>x</sub> formation is determined by the Zeldovich mechanism [42]. It is formed by the reactions between molecular oxygen and nitrogen, and is highly preferred under high combustion temperature. Since MILD combustion is featured as lower combustion temperature peak, the contribution of thermal-NO<sub>x</sub> to the final emission would be weakened.

The prompt-NO<sub>x</sub> is formed by the reactions between molecular nitrogen and hydrocarbon radicals especially under fuel-rich condition. For conventional combustion, prompt-NO<sub>x</sub> formation is usually ignored as compared to other paths. While under MILD combustion, this role would be strengthened, since a more reductive atmosphere is created under MILD combustion.

The fuel-NO<sub>x</sub> is formed by the oxidation of N element contained in the fuel itself. For coal combustion, the element N is distributed in both char and volatiles, the simplified formation path of fuel-NO<sub>x</sub> is shown in Fig. 1 [25]. Specifically, the N contained in char (Char-N) is converted to NO directly, while the N contained in volatiles (Vol-N) is converted to HCN first, and then HCN is oxidized to NO or reduced to N<sub>2</sub>, respectively. During coal combustion, this route accounts for most of the NO<sub>x</sub> emission. Hence, this mechanism seems to dominate the final NO<sub>x</sub> emission, since thermal-NO<sub>x</sub> is highly reduced under MILD combustion.

In addition, because the atmosphere under MILD combustion is more reductive, the generated NO<sub>x</sub> can be reduced by the gaseous hydrocarbons as well as the char particle through [25]:



$$\frac{d[\text{NO}]}{dt} = -A \exp\left(-\frac{E}{RT_p}\right) A_c P_{\text{NO}} \quad (3)$$

Table 4

Experimental conditions in IFRF's experiment [21].

	Mass flow (kg/h)	Temperature (K)	Enthalpy (MW)	Composition (wt%, wet)
Coal	66		0.58	
Primary air	130	313	–	O <sub>2</sub> = 23; N <sub>2</sub> = 77
Secondary air	675	1623	0.30	O <sub>2</sub> = 22; H <sub>2</sub> O = 9.5; CO <sub>2</sub> = 12.5; N <sub>2</sub> = 56; NO = 89 × 10 <sup>−4</sup>

**Table 5**  
Parameters of the coal particle size distribution [21].

Parameter	Value	Unit
Mean diameter	42	$\mu\text{m}$
Max. diameter	300	$\mu\text{m}$
Min. diameter	10	$\mu\text{m}$
Spread parameter	1.36	

**Table 6**  
Computational conditions of the considered cases in the present study.

Cases	Feed gas composition (vol. %)			Mass flow rate (kg/s)		
	O <sub>2</sub>	N <sub>2</sub>	CO <sub>2</sub>	Primary stream	Secondary stream	coal
AM	21	79	/	0.037	0.149	0.0183
OM21	21	/	79	0.055	0.222	0.0183
OM24	24	/	76	0.047	0.190	0.0183
OM27	27	/	73	0.041	0.165	0.0183
OM30	30	/	70	0.036	0.146	0.0183

where  $A = 4.18 \times 10^{-4} [\text{mol}/(\text{m}^2 \text{ s Pa})]$ ,  $E/R = 17,500 \text{ K}$ ,  $A_c$  is the total surface area of the char particle ( $\text{m}^2$ ), and  $P_{\text{NO}}$  is the NO partial pressure (Pa).

### 2.3. Physical configurations and computational conditions

The present simulation work is based on the experimental study of coal MILD combustion conducted in IFRF [19–21,23]. Fig. 2 shows the furnace and burner configurations used in the experiment. The furnace chamber is characterized by a square section of  $2 \times 2 \text{ m}$  and a total length of 6.25 m. The burner consisted of a central inlet for secondary stream and two side inlets for primary stream (coal and carrier gas), with a fuel input of 0.58 MW. Owing to the symmetrical structure of the experimental furnace, only one quarter is modeled to reduce the cost of the simulations. The computational grid is composed of about 500,000 hexahedral cells (see Fig. 3). Near the inlet regions, there are size functions to control the growth of the cell size. First, the whole computational domain is divided into several blocks, and then each block is meshed respectively. In order to show that the present solution

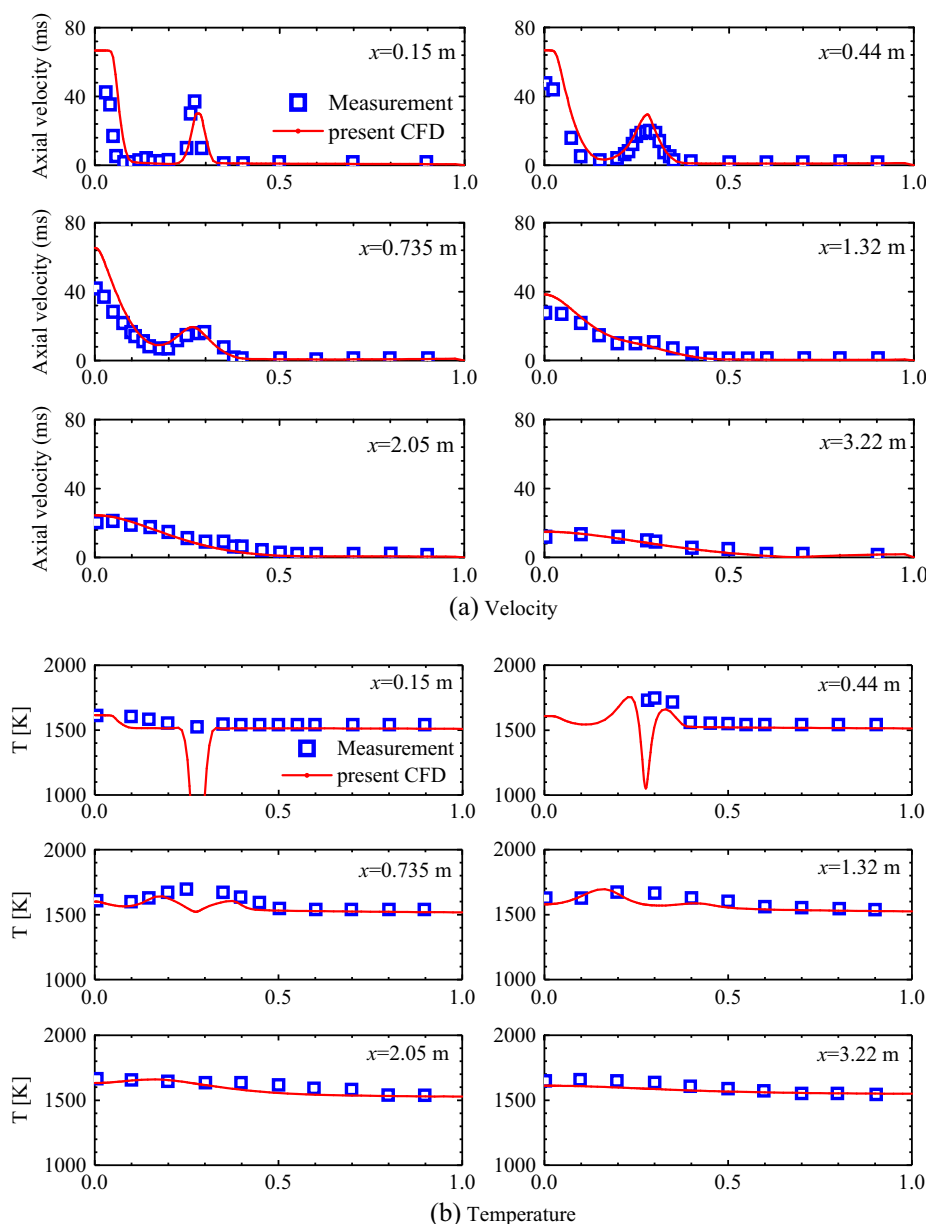


**Fig. 5.** Simulated and experimental results of the reference case for model validation.

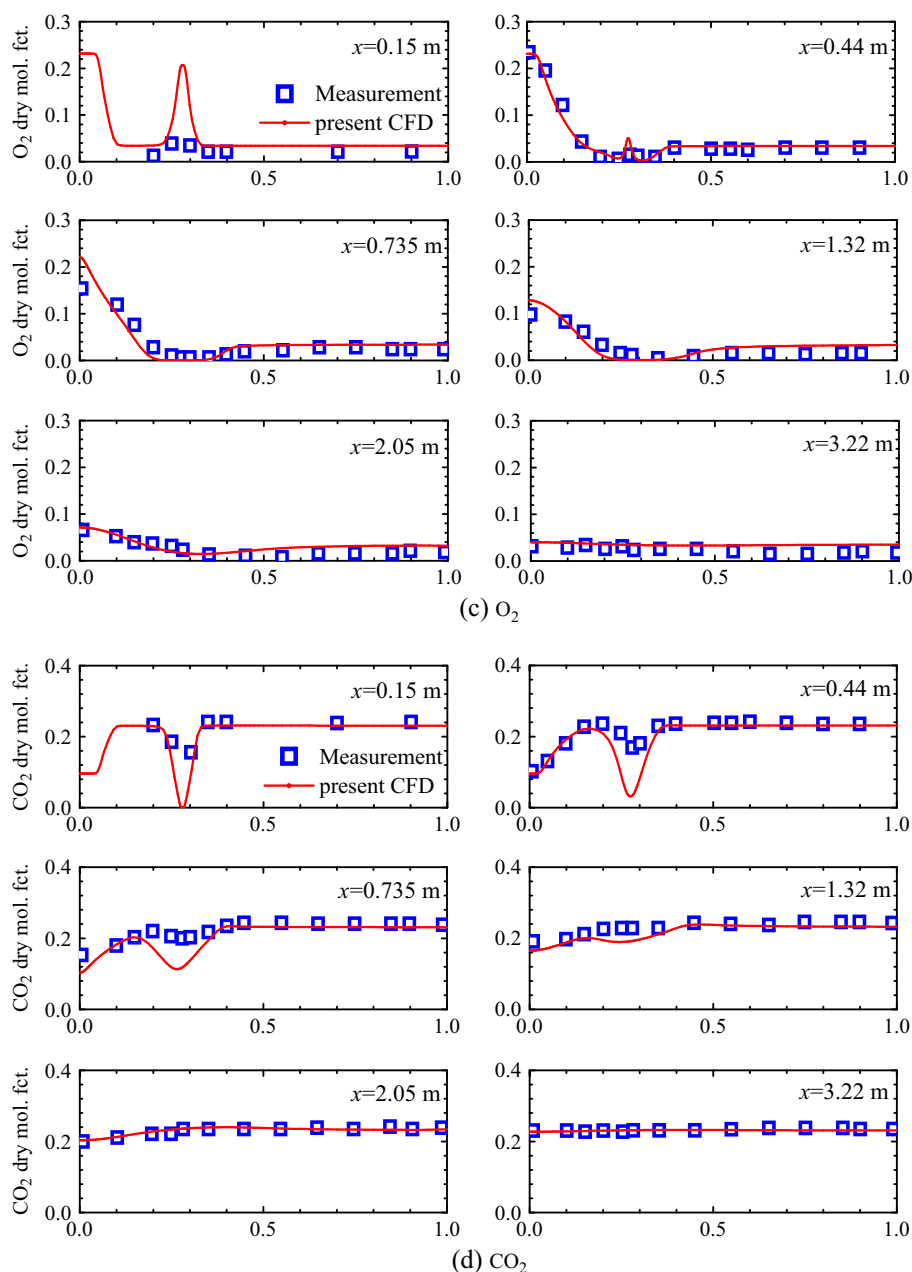


Fig. 5 (continued).

is independent with the grid, a finer grid with about 1,300,000 cells is used for modeling case AM. Fig. 4 shows the comparison of axial temperature and velocity distributions between the two grids. No obvious distinction can be found, hence, the coarse grid with about 500,000 cells is utilized to reduce the computational cost.

In IFRF's experiment, the secondary stream is preheated up to 1623 K by means of adding pure oxygen into combustion products from a pre-combustor. Therefore, there are other species (e.g.  $CO_2$ ,  $H_2O$ ) in addition to  $O_2$  and  $N_2$  in the oxidizer. Tables 4 and 5 give the detailed conditions of the IFRF experiment and parameters of the coal particle size distribution, respectively. As can be seen, there exists a certain amount of  $NO$  in the high temperature air, which may bring adverse effects on the evaluating of  $NO_x$  formation. In order to eliminate the uncertain impacts of the initial species on the final production, especially  $NO_x$  formation,  $O_2/N_2$  and  $O_2/CO_2$  are used as oxidizers

for air-fired and oxy-fired combustion, respectively. Table 6 summarizes the inlet conditions for the considered cases in the present study. Worth noting that, the inlet temperature of primary and secondary streams is kept consistent with the experimental condition for the MILD combustion cases as well as the fuel thermal input, and the excess oxygen coefficient is fixed at 1.2 in all cases.

### 3. Results and discussion

In this section, the validation of the present adopted models in modeling coal MILD combustion is carried out for the IFRF's experiment [19–21,23] first. Then, the combustion characteristics were comprehensively compared between air-MILD combustion (case AM) and oxy-MILD combustion (cases OM) in terms of temperature distribution, species distributions and  $NO_x$  formation.



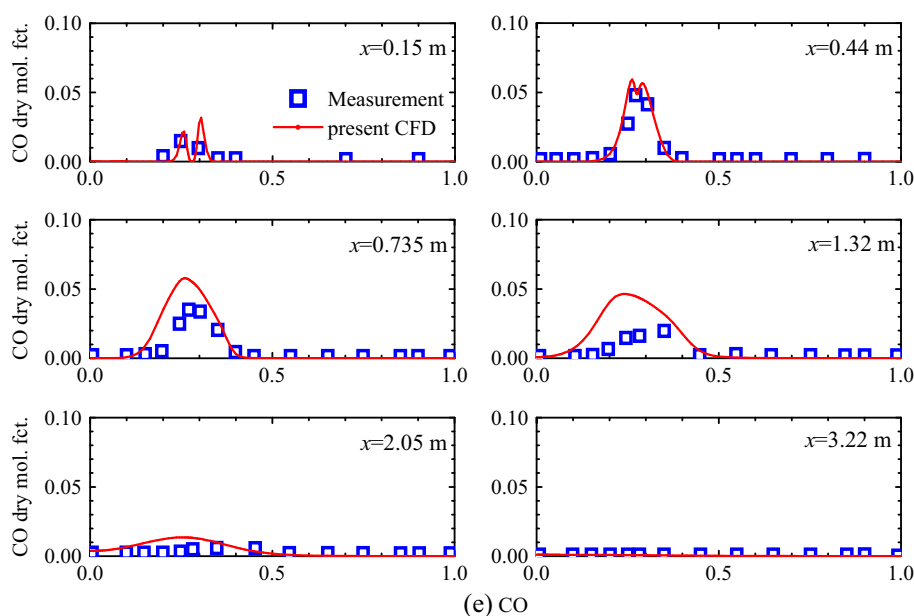


Fig. 5 (continued).

### 3.1. Model validation

In order to examine the adequacy of the adopted models on modeling coal MILD combustion, the simulated results of mean velocity, temperature distribution,  $O_2$ ,  $CO_2$  and CO concentrations in furnace were compared with the experimental data at different measurement locations (see Panels a–e of Fig. 5). In Fig. 5(a), the simulated velocity in the central

region is found to be lower than the measured results at the upper three traverses. As indicated by Orsino et al. [19] and Schaffel et al. [22], this distinction is caused by the poor laser Doppler anemometer (LDA) measurement. As for temperature (see Fig. 5(b)) and species (see Fig. 5(c–e)) distributions, imperfections are observed in the fuel region. This partly reflects that the coal ignition is delayed in the present simulation. However, this unsatisfactory prediction is also within observation in

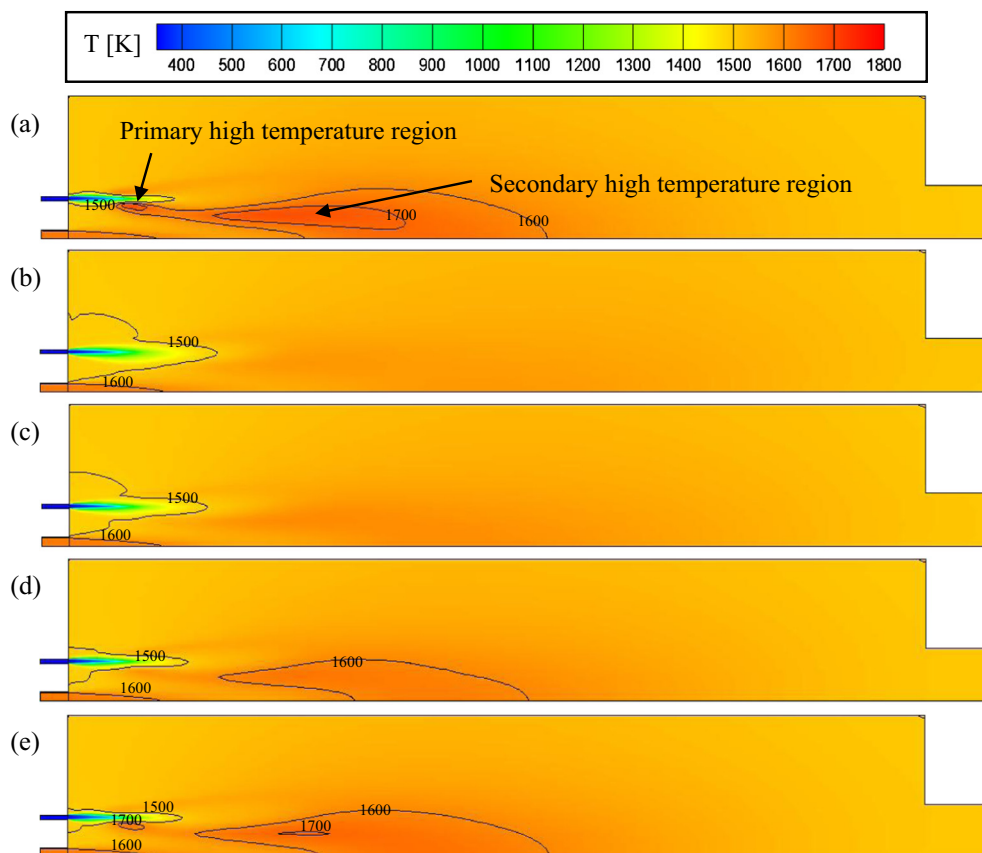


Fig. 6. Temperature distributions in the x–y plane for cases: (a) AM, (b) OM21, (c) OM24, (d) OM27 and (e) OM30.

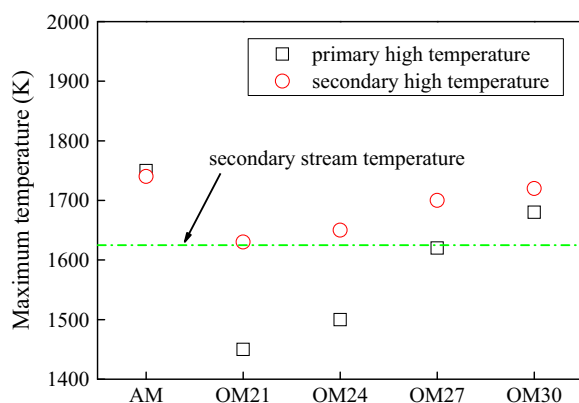


Fig. 7. Maximum temperature in primary and secondary high temperature regions for AM and OM cases.

the simulations by Scheffel et al. [22], Vascellari et al. [23] and Mei et al. [43]. Nevertheless, the present simulation utilizes the maximum steps of global reaction mechanism on coal MILD combustion so far together with the EDC combustion model, and the simulation results for the above parameters both quantitatively and qualitatively agree well with the experimental results. Hence, these methods are acceptable and continued to be applied in the subsequent simulations.

### 3.2. Combustion characteristics between AM and OM

#### 3.2.1. Temperature distribution

Fig. 6 compares the temperature fields in the x–y plane between air-MILD combustion (case AM) and oxy-MILD combustion (cases OM). Quite uniform temperature distribution is obtained with the maximum

temperature lower than 1800 K for all the combustion cases. Specifically, for case AM, two local high temperature regions are observed in the upstream furnace, namely the primary and secondary high temperature region as indicated in Fig. 6(a). In the primary high temperature region, the volatiles start to release from the coal particle due to the preheating by the entrained hot flue gas, and then react with oxygen to form the high temperature region. In the mixing region where the primary stream meets the secondary stream, the remained char in coal particles continues to react with oxygen in the secondary stream region. Therefore, the secondary high temperature region is formed.

However, the appearance of the local high temperature regions becomes less obvious under the present OM cases, especially at lower initial oxygen concentration. This is caused by the enhanced momentum of oxidizer in OM cases, which improves the internal recirculation, and further brings a negative effect to the mixing between primary and secondary streams. Consequently, the cold primary stream penetrates to a further distance which can be inferred by the isotherm of 1500 K. Note that, Schaffel et al. [22] found the combustion temperature peak is significantly suppressed when the central air velocity is increased from 60 to 120 m/s in their boiler design using MILD technology, and claimed that if the injection velocity is reduced by half, the internal recirculation would be not intensive enough. This is also observed for the secondary high temperature distribution with varied injection velocity in the study of Mei et al. [43] While in fact, changing the injection velocity or oxidizer components plays the approximate role as changing the injection momentum, which has an important impact on the in-furnace dynamic flow field.

Fig. 7 presents the maximum temperatures in the primary and secondary regions of each case, and the oxygen concentration seems to show a greater impact on the primary high temperature under OM conditions. With the improvement of oxygen concentration in the OM cases, the injection momentum of oxidizer gradually reduces due to the removal of CO<sub>2</sub>. Hence, the weakened internal recirculation results

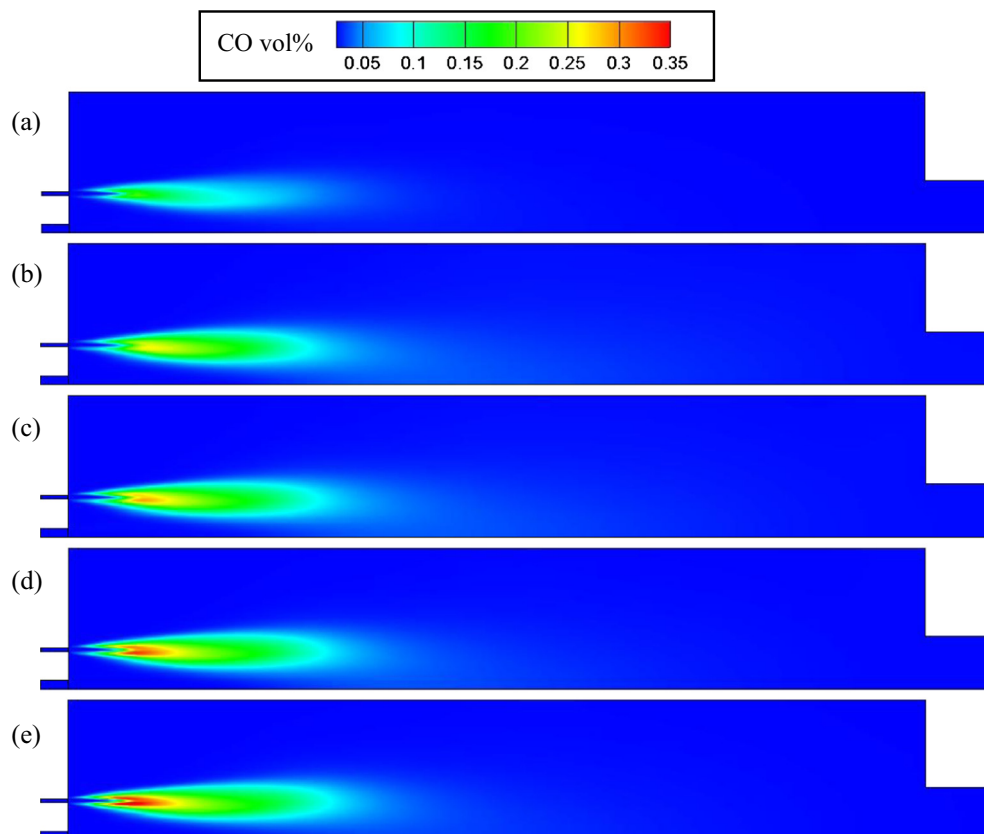


Fig. 8. CO distributions in the x–y plane for cases: (a) AM, (b) OM21, (c) OM24, (d) OM27 and (e) OM30.

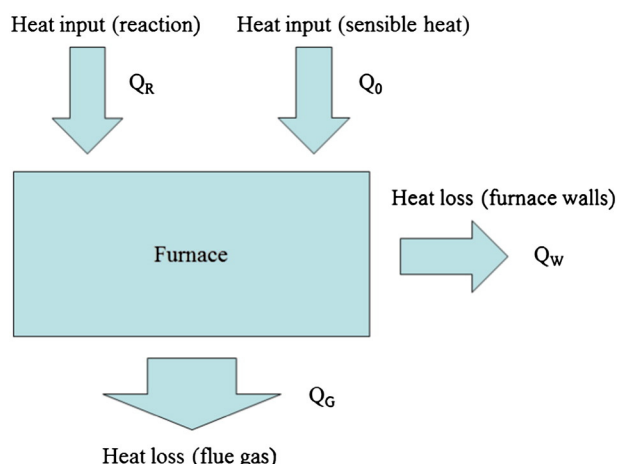


Fig. 9. Heat balance in the present combustion system.

in a higher combustion temperature in both primary and secondary regions. Until case OM27, the temperature distribution seems to be similar to case AM, since the injection momentum under the two cases is approximate to each other. However, even though when the oxygen concentration is enhanced to 30%, the temperature level of case OM30 is found to be still lower than case AM. This is different from the conventional combustion situation, in that to obtain a similar combustion temperature level to air combustion using a conventional burner, the oxygen concentration just needs to be enhanced to 27%–30% for oxy-fuel combustion. This distinction is expected to result mainly from the different reaction rates between conventional and MILD combustion. In particular, conventional combustion is usually applied with swirl burner, which promotes the mixing of reactants, and the reaction rate is improved accordingly. While MILD combustion is featured as intense recirculation, which leads to distributed species and slower reaction rate. Therefore, the temperature rise is less sensible to the oxygen concentration improvement under MILD condition as compared to that under conventional condition.

### 3.2.2. Species distribution

Fig. 8 displays the CO distributions in the x–y plane for air-MILD combustion (case AM) and oxy-MILD combustion (cases OM) at varied oxygen concentration. In case AM, the CO release concentration appears to be much lower than the OM cases. Specifically, the maximum CO concentration in case AM is lower than 10%, while it exceeds 20% for all OM cases. Moreover, with the increase of oxygen concentration under oxy-MILD conditions, the CO release peak shows a rising trend. When the oxygen concentration is enhanced to 30%, the CO release peak reaches as high as 35%.

According to the present reaction mechanism (see Table 3), CO forms from mainly the oxidation of coal and the conversions of intermediates. As for the reactions relevant to CO<sub>2</sub>, e.g. R.2, R.3 and R.5, the high CO<sub>2</sub> partial pressure under oxy-fuel condition leads to a negative effect on the CO oxidation. Hence, the CO release peak under oxy-fuel condition is expected to be higher than air condition. In addition, under OM conditions, the oxygen enhancement causes higher CO release due to the accelerated pyrolysis of coal under higher combustion temperature level.

For the present combustion system, the heat balance is represented as Fig. 9. According to the energy conservation principle, the following relationship can be obtained:

$$Q_R + Q_0 = Q_W + Q_G \quad (4)$$

where  $Q_R$  and  $Q_0$  stand for the heat input from chemical reaction and physical sensible heat, and  $Q_W$  and  $Q_G$  stand for the heat loss on the furnace walls and in the flue gas, respectively. Note that, the values of  $Q_0$ ,  $Q_W$  and  $Q_G$  can be obtained from the CFD calculation, and  $Q_R$  is then available by heat balance calculation.

Fig. 10 shows the heat release ratio and CO emission of the present cases. Note that, the heat release ratio is characterized as a ratio between the released reaction heat ( $Q_R$ ) and the fuel input (580 KW). It can be found that case AM has the largest heat release together with the lowest CO emission. At the same time, under OM conditions, the heat release increases while CO emission reduces when enhancing the oxygen concentration. In addition, the lower heat release and larger CO emission seem to be another reason for the reduced temperature level for OM cases. Worth noting that, the coal burnout can be reflected by the heat release ratio. Concretely, the higher heat release ratio represents the better coal burnout. Therefore, the coal burnout is weakened when replacing N<sub>2</sub> by CO<sub>2</sub>, and the oxygen concentration under OM condition needs to be above 30% to achieve the same burnout as air condition, which is consistent to the observation of temperature distribution.

Fig. 11 displays the O<sub>2</sub> distributions in the x–y plane for air-MILD combustion (case AM) and oxy-MILD combustion (cases OM). The O<sub>2</sub> field in each case shows a common feature that the O<sub>2</sub> concentration (by volume) is lower than 10% in most of the furnace. Simultaneously, in order to represent the low oxygen dilution characteristic under MILD operation, the area where the local oxygen concentration is lower than 1% is also depicted in Fig. 11.

For OM cases, the low oxygen area is found to be expanded when increasing the oxygen concentration in oxidizer (see Fig. 11(b–e)). The reasons behind this may be that: 1) The injection momentum drops when improving oxygen concentration and hence the internal recirculation is weakened. As a result, the mixing between the reactants becomes better due to destructive dilution, and hence the combustion rate as well as the oxygen consumption is promoted. 2) According to the CO distribution, larger CO release is obtained due to accelerated pyrolysis of coal. Thus, the oxygen consumption is increased. As a result, the low oxygen area is enlarged with the enhancement of initial oxygen concentration.

According to Fig. 11, case AM is found to have the largest low oxygen area among the present cases. Apart from the above reasons, the molecular diffusion may make some difference. As indicated by A. Mardani et al. [44], the molecular diffusion in MILD combustion has a comparable effect with the turbulent transport. In this regard, the oxygen molecular gains a larger diffusion rate in O<sub>2</sub>/N<sub>2</sub> than O<sub>2</sub>/CO<sub>2</sub> [41]. Hence, the combustion rate is expected to be higher in case AM than cases OM, even though the injection momentum of case AM is approximate to case OM27. Consequently, the low oxygen area in case AM is larger than OM cases.

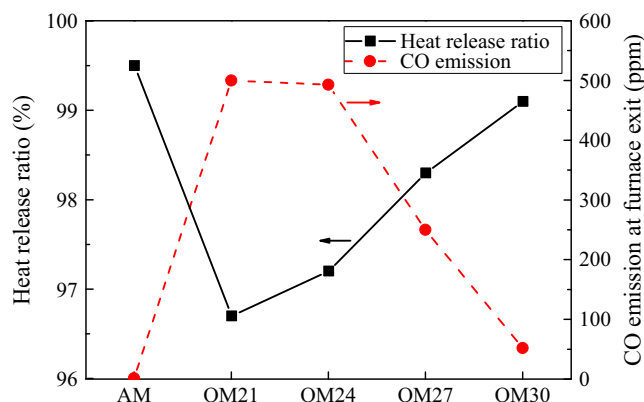


Fig. 10. Heat release ratio and CO emission of the present cases.



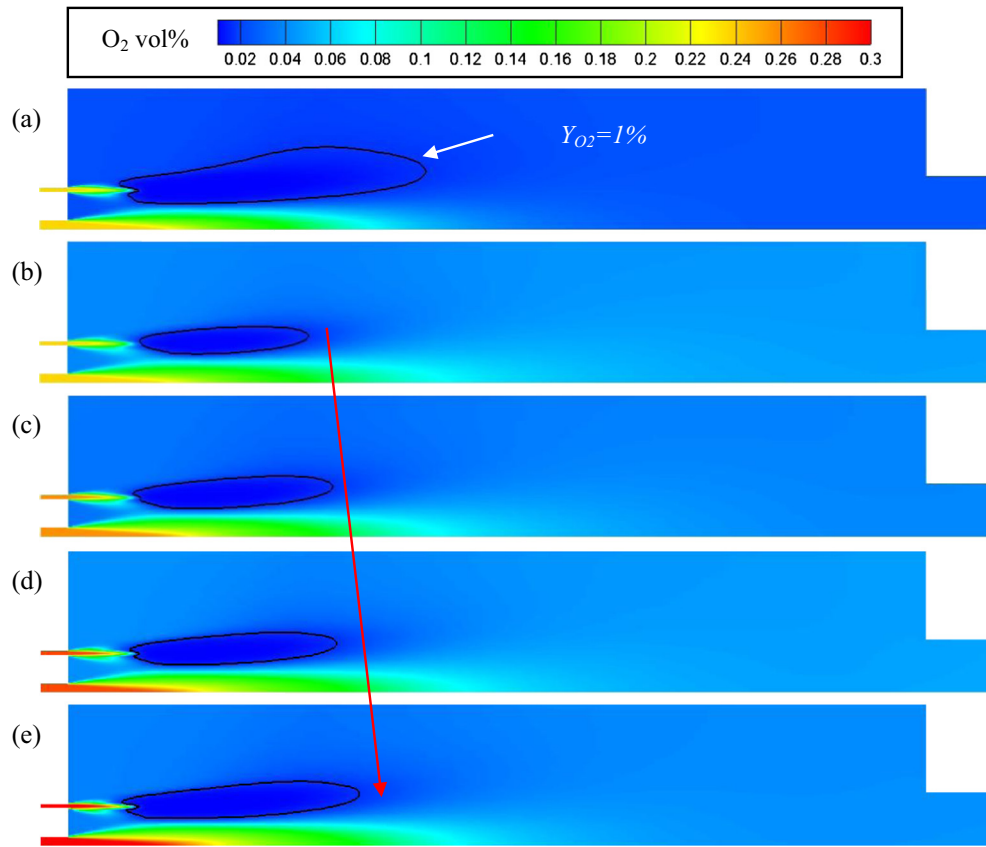


Fig. 11. O<sub>2</sub> distributions in the x–y plane for cases: (a) AM, (b) OM21, (c) OM24, (d) OM27 and (e) OM30.

### 3.2.3. NO<sub>x</sub> conversion

For gaseous fuels, like CO, H<sub>2</sub> and CH<sub>4</sub>, the generated NO<sub>x</sub> mainly comes from the thermal route, which is favored in condition of high temperature. As is known, the combustion temperature peak can be significantly suppressed under MILD combustion due to the intense recirculation inside the furnace. By this means, the thermal NO<sub>x</sub> formation can be extremely low under MILD operation. However, for N-contained fuels, such as coal and biomass, the N element can be converted directly or indirectly into NO during the combustion process, which is stated as fuel-NO<sub>x</sub> in Section 2.2. Moreover, the produced NO<sub>x</sub> from fuel-route plays the most important role in the final NO<sub>x</sub> emission for coal combustion. Especially under MILD combustion, since thermal-NO<sub>x</sub> is highly suppressed, the total NO<sub>x</sub> emission would be hence dominated by the fuel-NO<sub>x</sub> route. Furthermore, due to the absence of N<sub>2</sub> under oxy-MILD combustion, the thermal NO<sub>x</sub> formation is completely prevented. Worth noting that, during coal combustion, in addition to thermal-NO<sub>x</sub> and fuel-NO<sub>x</sub>, prompt-NO<sub>x</sub> can also form. However, this route is usually negligible as compared to the thermal-NO<sub>x</sub> and fuel-NO<sub>x</sub> route. Therefore, in the present work, only the fuel-NO<sub>x</sub> is taken into consideration for the considered cases.

Because of the different flow rate at the furnace exit for each case, the NO<sub>x</sub> emission concentration is not sufficient to precisely evaluate the fuel-NO<sub>x</sub> formation. Therefore, the concept of fuel-N conversion ratio is used to characterize the fuel-NO<sub>x</sub> formation, which is calculated by:

$$R_N = \frac{w_{NO}(m_{pri} + m_{sec} + m_{coal}B)M_N}{w_{NO}m_{coal}BM_{NO}} \quad (5)$$

where,  $w_{NO}$  is the NO mass fraction at the furnace exit;  $m_{pri}$ ,  $m_{sec}$ , and  $m_{coal}$  stand for the mass flow rate of primary stream, secondary stream

and coal, respectively;  $w_N$  means the mass fraction of N in coal particle;  $B$  is the coal burnout degree;  $M_N$  and  $M_{NO}$  represent the molecular mass of N and NO, respectively. Note that, the coal burnout degree is also regarded as a parameter of the combustion characteristic. Even though lower burnout degree is obtained for OM cases according to the heat release ratio, it seems to play a minor role for the considered cases in the present simulations. Therefore, it is not further discussed in this paper.

Fig. 12 shows the fuel-N conversion ratio for the present cases. The oxy-MILD combustion (cases OM) seems to have a greater potential on NO<sub>x</sub> reduction than the air-MILD combustion (case AM). Moreover, with the enhancement of oxygen concentration in oxidizer under oxy-MILD conditions, the fuel-N conversion ratio keeps falling from 10.3% to 4.4%. The reason behind this can be explained by: (1) Under

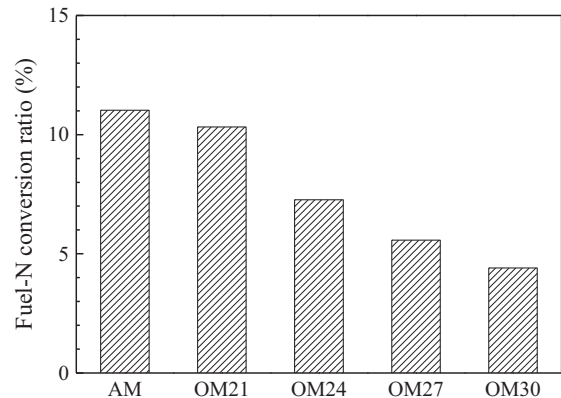


Fig. 12. Fuel-N conversion ratio for AM and OM cases.

oxy-MILD combustion, the higher CO release would bring a positive effect on the formation of the intermediates, i.e.  $\text{CH}_i$ . These intermediates can then react with NO through Eq. (2). Hence, the oxy-MILD combustion is preferable than air-MILD combustion on  $\text{NO}_x$  reduction. (2) According to the CO release in Fig. 8, it can be inferred that the release of volatiles is also facilitated with the enrichment of oxygen in oxidizer. Meanwhile, based on the fuel- $\text{NO}_x$  formation path (see Fig. 1), the char-N is converted to NO directly, while the volatiles-N is converted to HCN first. Thus, the conversion of volatiles-N to HCN is promoted, while the direct oxidation of char-N is weakened. In addition, the N in HCN can be converted to NO and  $\text{N}_2$  respectively as Eqs. (6) and (7) show. According to He et al. [25], the high release of HCN would cause the fast generation of NO, but the high HCN and NO concentration together would make NO destruction rapidly. In the present study, the formation and destruction of NO reach equilibrium with HCN under oxy-MILD combustion. As a result, the fuel- $\text{NO}_x$  conversion ratio decreases with oxygen enhancement.



#### 4. Conclusions

This paper investigates the MILD combustion characteristics of coal in  $\text{O}_2/\text{N}_2$  and  $\text{O}_2/\text{CO}_2$  atmospheres with the aid of CFD modeling. Simplified mechanism containing homogeneous volumetric reaction as well as heterogeneous surface reaction is used to simulate the combustion of coal together with the EDC model. With the adopted modeling methods, the simulated results agree well with the experimental measurements for the reference case. A comprehensive comparison is made in terms of temperature distribution, species distribution, and  $\text{NO}_x$  conversion between air-MILD combustion and oxy-MILD combustion. Findings and conclusions can be drawn as follows:

1. With the enhancement of oxygen concentration in initial oxidizer, the temperature level under oxy-MILD combustion increases gradually due to the weakened injection momentum and promoted heat release.
2. With the enhancement of oxygen concentration in initial oxidizer, the in-furnace CO release increases while its final emission reduces under oxy-MILD combustion.
3. The oxy-MILD combustion shows a greater potential on  $\text{NO}_x$  reduction than the air-MILD combustion. When improving the  $\text{O}_2$  level under oxy-MILD combustion, the conversion of fuel-N into  $\text{NO}_x$  is suppressed.

#### Acknowledgments

This work was supported by National Natural Science Foundation of China (51276074), State Key Development Program for Basic Research of China (2011CB707301) and Doctoral Fund of Ministry of Education of China (20130142130009).

#### References

- [1] A. Cavaliere, M. de Joannon, Mild combustion, *Progress in Energy and Combustion Science* 30 (2004) 329–366.
- [2] M. Katsuki, T. Hasegawa, The science and technology of combustion in highly preheated air, *Proceedings of the Combustion Institute* 27 (1998) 3135–3146.
- [3] J.A. Wünnig, J.G. Wünnig, Flameless oxidation to reduce thermal NO-formation, *Progress in Energy and Combustion Science* 23 (1997) 81–94.
- [4] P.F. Li, J.C. Mi, B.B. Dally, F.F. Wang, L. Wang, Z.H. Liu, S. Chen, C.G. Zheng, Progress and recent trend in MILD combustion, *Science China Technological Sciences* 54 (2011) 255–269.
- [5] K. Narayanan, W. Blasiak, A. Lugnet, Development of high temperature air and oxyfuel combustion technologies for minimized  $\text{CO}_2$  and  $\text{NO}_x$  emissions in industrial

- heating, Joint International Conference on “Sustainable Energy and Environment”, Hua Hin, Thailand, 2004.
- [6] K. Narayanan, W. Wang, W. Blasiak, T. Ekman, Flameless oxyfuel combustion: technology, modelling and benefits in use, *Revue de Metallurgie* 103 (2006) 210–217.
- [7] W. Blasiak, W.H. Yang, K. Narayanan, J. von Scheele, Flameless oxyfuel combustion for fuel consumption and nitrogen oxides emissions reductions and productivity increase, *Journal of the Energy Institute* 80 (2007) 3–11.
- [8] C. Villermaux, S. Maurel, T. Hortanet, T. Bellin-Croyat, T. Ferlin, Flameless oxy-FGR: An Energy Efficient Combustion Concept that Complies with Environmental Regulation and Offers Direct  $\text{CO}_2$  Capture Solution for Existing and New Gas Furnaces, 24th World Gas Conference, 2009.
- [9] C. Villermaux, L. Porcheron, N. Richard, S. Carpentier, R. Hauguel, A. Quinqueneau, GDF SUEZ activities on flameless combustion: from physical phenomena analysis to industrial-scale applications, International Gas Union Research Conference, 2008.
- [10] H. Tsuji, A. Gupta, T. Hasegawa, High Temperature Air Combustion: From Energy Conservation to Pollution Reduction, CRC Press, Florida, 2003.
- [11] J. Wünnig, Flameless Oxidation, 6th HiTAC Symposium-2005, Essen, Germany, 2005.
- [12] S. Chen, J.C. Mi, H. Liu, C.G. Zheng, First and second thermodynamic-law analyses of hydrogen-air counter-flow diffusion combustion in various combustion modes, *International Journal of Hydrogen Energy* 37 (2012) 5234–5245.
- [13] A. Parente, C. Galletti, J. Riccardi, M. Schiavetti, L. Tognotti, Experimental and numerical investigation of a micro-CHP flameless unit, *Applied Energy* 89 (2012) 203–214.
- [14] B. Danon, E.-S. Cho, W. de Jong, D. Roekaerts, Numerical investigation of burner positioning effects in a multi-burner flameless combustion furnace, *Applied Thermal Engineering* 31 (2011) 3885–3896.
- [15] P.R. Medwell, B.B. Dally, Effect of fuel composition on jet flames in a heated and diluted oxidant stream, *Combustion and Flame* 159 (2012) 3138–3145.
- [16] J.C. Mi, P.F. Li, C.G. Zheng, Impact of injection conditions on flame characteristics from a parallel multi-jet burner, *Energy* 36 (2011) 6583–6595.
- [17] M. de Joannon, G. Sorrentino, A. Cavaliere, MILD combustion in diffusion-controlled regimes of hot diluted fuel, *Combustion and Flame* 159 (2012) 1832–1839.
- [18] R. Weber, A.L. Verlaan, S. Orsino, N. Lallemand, On emerging furnace design methodology that provides substantial energy savings and drastic reductions in  $\text{CO}_2$ ,  $\text{CO}$  and  $\text{NO}_x$  emissions, *Proceedings of 5th European Conference on Industrial Furnaces and Boilers*, Lisbon, Portugal, 2000.
- [19] S. Orsino, M. Tamura, P. Stabat, S. Costantini, O. Prado, R. Weber, Excess enthalpy combustion of coal, Technological Report IFRF Doc. No. F46/y/3, IFRF, 2000.
- [20] R. Weber, J. Smart, W. vd Kamp, On the (MILD) combustion of gaseous, liquid, and solid fuels in high temperature preheated air, *Proceedings of the Combustion Institute* 30 (2005) 2623–2629.
- [21] N. Schaffel, M. Mancini, A. Szlek, R. Weber, Mathematical modelling of MILD combustion of pulverized coal, *Combustion and Flame* 156 (2009) 1771–1784.
- [22] N. Schaffel, M. Mancini, A. Szlek, R. Weber, Novel conceptual design of a supercritical pulverized coal boiler utilizing high temperature air combustion (HTAC) technology, *Energy* 35 (2010) 2752–2760.
- [23] M. Vascellari, G. Cau, Influence of turbulence-chemical interaction on CFD pulverized coal MILD combustion modelling, *Fuel* 101 (2012) 90–101.
- [24] T. Suda, M. Takafuji, T. Hirata, A study of combustion behavior of pulverized coal in high temperature air, *Proceedings of the Combustion Institute* 29 (2002) 503–509.
- [25] R. He, T. Suda, M. Takafuji, Analysis of low NO emission in high temperature air combustion for pulverized coal, *Fuel* 83 (2004) 1133–1141.
- [26] D. Ristic, A. Schuster, G. Scheffknecht, H. Stadler, M. Förster, R. Kneer, Experimental study on flameless oxidation of pulverized coal in bench and pilot scale, *Proceedings of the 23th German Flameday*, Berlin, Germany, 2007.
- [27] D. Ristic, M. Schneider, A. Schuster, Investigation of  $\text{NO}_x$  formation for flameless coal combustion, 7th High Temperature Air Combustion and Gasification International Symposium, Phuket, Thailand, 2008.
- [28] H. Stadler, D. Ristic, M. Förster,  $\text{NO}_x$ -emissions from flameless coal combustion in air,  $\text{Ar}/\text{O}_2$  and  $\text{CO}_2/\text{O}_2$ , *Proceedings of the Combustion Institute* 32 (2009) 3131–3138.
- [29] H. Stadler, D. Toporov, M. Förster, On the influence of the char gasification reactions on NO formation in flameless coal combustion, *Combustion and Flame* 156 (2009) 1755–1763.
- [30] H.A. Stadler, Experimental and Numerical Investigation of Flameless Pulverized Coal Combustion Ph.D. thesis Mechanical Engineering of the RWTH2010.
- [31] H. Stadler, D. Christ, M. Habermeh, P. Heil, A. Kellermann, Experimental investigation of  $\text{NO}_x$  emissions in oxycoal combustion, *Fuel* 90 (2011) 1604–1611.
- [32] H. Zhang, G.X. Yue, J. Lu, Z. Jia, J. Mao, T. Fujimori, T. Suko, T. Kiga, Development of high temperature air combustion technology in pulverized fossil fuel fired boilers, *Proceedings of the Combustion Institute* 31 (2007) 2779–2785.
- [33] C.J. Tang, M. Fang, Z.G. Tang, Experimental study on the oxy-fuel flameless combustion of pulverized coal, *Power System Engineering* 26 (2010) 8–10 (in Chinese).
- [34] B.B. Dally, S.H. Shim, R.A. Craig, On the burning of sawdust in a MILD combustion furnace, *Energy & Fuels* 24 (2010) 3462–3470.
- [35] Y.J. Tu, H. Liu, P.F. Li, F.F. Wang, T. Zhang, C. Bai, Y. Zheng, Z.H. Liu, J.C. Mi, C.G. Zheng, Experimental study of MILD combustion for pulverized coal in 0.3 MW vertical furnace, 9th Asia-Pacific Conference on Combustion, Gyeongju, Korea, 2013.
- [36] P. Li, F. Wang, Y. Tu, Z. Mei, J. Zhang, Y. Zheng, H. Liu, Z. Liu, J. Mi, C. Zheng, Moderate or intense low-oxygen dilution oxy-combustion characteristics of light oil and pulverized coal in a pilot-scale furnace, *Energy & Fuels* 28 (2014) 1524–1535.
- [37] ANSYS, Inc., Fluent 6.3 Documentation, ANSYS, Inc., Canonsburg, PA, 2007.
- [38] A.H. Al-Abbas, J. Naser, D. Dodds, CFD modelling of air-fired and oxy-fuel combustion of lignite in a 100 kW furnace, *Fuel* 90 (2011) 1778–1795.
- [39] S.R. Gubba, L. Ma, M. Pourkashanian, A. Williams, Influence of particle shape and internal thermal gradients of biomass particles on pulverized coal/biomass co-fired flames, *Fuel Processing Technology* 92 (2011) 2185–2195.

- [40] D. Förtsch, F. Kluger, U. Schnell, H. Spliethoff, K. Hein, A kinetic model for the prediction of no emissions from staged combustion of pulverized coal, *Proceedings of the Combustion Institute* 27 (1998) 3037–3044.
- [41] J.Z. Liu, S. Chen, Z.H. Liu, K. Peng, N. Zhou, X.H. Huang, T. Zhang, C.G. Zheng, Mathematical modelling of air and oxycoal confined swirling flames on two extended eddy-dissipation models, *Industrial & Engineering Chemistry Research* 51 (2012) 691–703.
- [42] Y.B. Zeldovich, P.Y. Sadvnikov, D.A. Frank-Kamenetskii, *Oxidation of Nitrogen in Combustion*, Publishing House of the Academy of Sciences, Moscow–Leningrad, USSR, 1947.
- [43] Z.F. Mei, P.F. Li, F.F. Wang, J.P. Zhang, J.C. Mi, Influences of reactant injection velocities on moderate or intense low-oxygen dilution coal combustion, *Energy & Fuels* 28 (2014) 369–384.
- [44] A. Mardani, S. Tabejamaat, M. Ghamari, Numerical study of influence of molecular diffusion in the Mild combustion regime, *Combustion Theory and Modelling* 14 (2010) 747–774.